INCOMPLETELY STIRRED REACTOR NETWORK MODELLING FOR SOOT EMISSIONS PREDICTION IN AERO-ENGINE COMBUSTORS

S. Gkantonas[1*], **A. Giusti**[2] **and E. Mastorakos**[1]

[1] Department of Engineering, University of Cambridge, UK

[2] Department of Mech. Engineering, Imperial College London, UK

[*]Correspondent author: sg834@cam.ac.uk

ABSTRACT

The simulation of soot from swirl flames is a problem of relevance for the development of low-emission aero-engine combustors. Apart from detailed CFD approaches, it is of importance to also develop models with modest computational cost so parametric studies can be performed, especially in view of the need to predict engine-out soot particle size distributions to meet future regulations. In this work, the Incompletely Stirred Reactor (ISR) equation is derived based on the Conditional Moment Closure combustion model. An ISR is a volume V that is inhomogeneous in terms of mixture fraction but is characterised by homogeneous conditional averages, such as temperature and soot mass fraction conditional on the mixture fraction having a particular value. A network of ISRs is then deployed to separately capture soot production and oxidation regions exhibiting different degrees of micro-mixing rates and residence times, as typically observed in rich-burn swirl flames with additional dilution air. The Incompletely Stirred Reactor Network (ISRN) approach is demonstrated on a calculation of the Cambridge Rich-Quench-Lean (RQL) combustor, where the residence time in the primary and secondary regions are controlled by the relative flow rates in the main annular swirl flow and the downstream dilution jets. The results show that the ISRN approach is computationally efficient and captures the experimentally observed soot tendency trends as a function of the burner operating conditions.

INTRODUCTION

The prediction of soot emissions and control of the particle sizes emitted from aero-engine combustors is of vital importance if next-generation engines are to mitigate the effects of particulate matter to human health and the environment [1]. The nature of soot evolution in turbulent flow, however, poses significant numerical challenges. Apart from an accurate knowledge of turbulent mixing and finite-rate chemistry effects, reliable predictions necessitate the use of complex soot models able to describe the underlying chemistry and the morphology of particles [2]. Predictions are known to be very sensitive to the choice of the soot model (e.g. [3]); therefore, sensitivity analysis and comparison between soot models are necessary to gain more insights into soot formation and oxidation. Nevertheless, comprehensive soot models cannot easily be used in conjunction with high-fidelity CFD simulations, given their high dimensionality and computational cost. Such attempts have only started to appear in the literature recently (e.g. [4, 5]), yet they cannot be easily employed in sensitivity analysis or during the design phase of aero-engine combustors. As a result, there is a motivation to develop computationally inexpensive methods which permit the use of complex soot models and the prediction of soot emissions within a reasonable degree of accuracy in both magnitude and trend.

In this direction, this study will introduce a new approach utilising an Incompletely Stirred Reactor Network (ISRN) to perform kinetic post-processing of CFD simulations. Due to its simplicity, this methodology allows for the use of comprehensive soot models with modest computational cost, while retaining approximate turbulence-chemistry interaction effects on the sooting flame structure. The Incompletely Stirred Reactor (ISR) model, initially investigated by Smith [6] and later developed by Mobini and coworkers [7, 8, 9], is a generalisation of the Perfectly Stirred Reactor. Its derivation is based on the Conditional Moment Closure (CMC) method for turbulent reacting flow [10] and can be viewed as a zero-dimensional approximation of CMC. An ISR is defined as a region of the flow, within which the flow and mixture fraction are inhomogeneous but conditional averages of reacting scalars, conditioned on the mixture fraction, are uniform. In the limit of strongly recirculating flow, far for extinction, ignition or highly-transient phenomena, the latter assumption allows for the use of simple ordinary differential equations in mixture fraction space to model a combustor in its entirety, hence reducing the total computational cost.

Notwithstanding that the ISR conditions are generally achieved in the primary zone of a highly efficient aero-engine combustor, conditional quantities related to soot evolution show strong spatial dependence, as discussed in Ref. [11, 12]. Therefore, it is necessary to extend the approach to a network of ISRs spanning the whole combustor under investigation. The combustor can then be partitioned in separate soot production and oxidation regions that exhibit different degrees of micro-mixing rates and residence times. In the context of kinetic post-processing, the ISRN equations can be decoupled from the calculation of the flow and mixing fields, consistently with other methods using ideal reactors (e.g. [13]). Unlike ideal reactors, however, turbulent mixing effects can be directly taken into account via the scalar dissipation rate and the mixture fraction probability density function (PDF). Their quantification is performed through averaging of the mixing field extracted from a reference CFD simulation.

The main objective of this study is to demonstrate the computational efficiency of the ISRN approach and its ability to describe soot evolution in aero-engine combustors. For this purpose, the ISRN approach is applied to the Cambridge model (RQL) combustor, previously characterised experimentally [14, 15, 16] and through high-fidelity simulations [5, 11, 12]. This extended abstract is structured as follows. The derivation of the ISRN equations is first introduced, followed by the solution strategy and a description of the investigated conditions. Preliminary results are presented next, followed by a discussion regarding the ISRN implementation. Main conclusions close the abstract.

MATHEMATICAL MODEL

An ISR is considered to be a volume V within which conditional averages of reacting scalars, conditioned on the mixture fraction, are independent of position and time. Various versions of the ISR governing equations have appeared in the literature [6, 7, 8, 9]. Here we extend the formulation given by Klimenko and Bilger [10] and derive the governing equations for a network of ISR reactors with an arbitrary number of inlet/outlet streams having non-uniform properties. The equations are derived from the CMC equation assuming high Reynolds number and negligible differential diffusion [10]:

$$\frac{\partial \overline{\rho} Q_\alpha \widetilde{P}_\eta}{\partial t} + \vec{\nabla}\cdot(\overline{\rho}\langle \vec{u} Y_\alpha|\eta\rangle \widetilde{P}_\eta) = \overline{\rho}\langle \dot{\omega}_\alpha|\eta\rangle \widetilde{P}_\eta - \frac{\partial^2 \overline{\rho}\langle N|\eta\rangle \widetilde{P}_\eta}{\partial \eta^2} Q_\alpha + \overline{\rho}\langle N|\eta\rangle \widetilde{P}_\eta \frac{\partial^2 Q_\alpha}{\partial \eta^2} \tag{1}$$

where η is the sample space variable of the mixture fraction, ξ, $Q_\alpha \equiv \langle Y_\alpha|\eta\rangle$ is the conditional average mass fraction of a generic species, $\widetilde{P}_\eta$ the Favre mean PDF and $N = D\vec{\nabla}\xi\cdot\vec{\nabla}\xi$ the scalar dissipation rate. Here, the angle brackets represent conditional density-weighted Favre averaging.

Considering statistically stationary flow, integration of Eq. (1) over the core volume and application of the flux divergence theorem to the LHS leads to:

$$\oint_A \overline{\rho}\langle \vec{u} Y_\alpha|\eta\rangle \widetilde{P}_\eta d\vec{A} = \int_V \left[\overline{\rho}\langle \dot{\omega}_\alpha|\eta\rangle \widetilde{P}_\eta - \frac{\partial^2 \overline{\rho}\langle N|\eta\rangle \widetilde{P}_\eta}{\partial \eta^2} Q_\alpha + \overline{\rho}\langle N|\eta\rangle \widetilde{P}_\eta \frac{\partial^2 Q_\alpha}{\partial \eta^2}\right] dV \tag{2}$$

By definition, conditional reactive scalar statistics are considered uniform inside an ISR core. Hence, they can be moved out of the integral on the RHS of Eq. (2). Moreover, conditional statistics are only a function of mixture fraction; therefore, their partial derivatives may be transformed into ordinary ones. Next, by introducing a diffusion approximation for the conditional correlations between species and velocity [10], assuming a turbulent diffusivity D_t equal for all scalars, the governing equation can be written in the following discrete form:

$$\sum_{i=1}^{F^{out}} (\dot{m}\widetilde{P}_\eta Q_\alpha)_i - \sum_{j=1}^{F^{in}} (\dot{m}\widetilde{P}_\eta Q_\alpha)_j + \sum_{i=1}^{F} \left(\overline{\rho} D_t (\vec{\nabla} Q_\alpha)\widetilde{P}_\eta \vec{A}\right)_i = V\rho^{**}\left[P_\eta^{**}\left(\dot{\omega}_\alpha|\eta + N_\eta^{**}\frac{d^2 Q_\alpha}{d\eta^2}\right) - Q_\alpha \frac{d^2 N_\eta^{**} P_\eta^{**}}{d\eta^2}\right] \tag{3}$$

where the core volume-averaged mass density, ρ^{**}, mixture fraction PDF, P_η^{**}, and scalar dissipation rate, N_η^{**} are defined by:

$$\rho^{**} \equiv \frac{1}{V}\int_V \overline{\rho} dV; \quad P_\eta^{**} \equiv \frac{1}{V\rho^{**}}\int_V \overline{\rho}\widetilde{P}_\eta dV; \quad N_\eta^{**} \equiv \frac{1}{V\rho^{**}P_\eta^{**}}\int_V \overline{\rho}\langle N|\eta\rangle P_\eta dV \tag{4}$$

Note the last term on the RHS of Eq. (3). To close this term, the transport equation for the mixture fraction PDF may be utilised [10]. Given a statistically stationary flow and neglecting molecular fluxes, the PDF equation becomes:

$$\vec{\nabla}\cdot(\overline{\rho}\langle \vec{u}|\eta\rangle \widetilde{P}_\eta) = -\frac{\partial^2 \overline{\rho}\langle N|\eta\rangle \widetilde{P}_\eta}{\partial \eta^2} \quad \Rightarrow \quad \sum_{i=1}^{F^{out}} (\dot{m}\widetilde{P}_\eta)_i - \sum_{j=1}^{F^{in}} (\dot{m}\widetilde{P}_\eta)_j = -V\rho^{**}\frac{d^2 N_\eta^{**} P_\eta^{**}}{d\eta^2} \tag{5}$$

where the flux divergence theorem and the definitions of Eq. (4) are employed. Consistently with the stirred reactor concept, the conditional quantities exiting the ISR may be taken equal to conditional quantities in the core. However, it is not necessary to assume that the outlet streams PDF is identical to the core [9]. Finally, the combination of Eq. (3)-(5) leads to the governing equation of an ISRN element:

$$\frac{1}{V\rho^{**}P_\eta^{**}}\left[\sum_{j=1}^{F^{in}} \left(\dot{m}\widetilde{P}_\eta\right)_j \left[Q_\alpha - (Q_\alpha)_j\right] + \sum_{i=1}^{F} \left(\overline{\rho} D_t (\vec{\nabla} Q_\alpha)\widetilde{P}_\eta \vec{A}\right)_i\right] = \langle \dot{\omega}_\alpha|\eta\rangle + N_\eta^{**}\frac{d^2 Q_\alpha}{d\eta^2} \tag{6}$$

SOLUTION STRATEGY

The ISRN approach starts with the creation of a standard computational grid and the calculation of the reacting flow field using CFD. The ISRN equations are then solved using an in-house unstructured finite volume code, initially developed for LES-CMC modelling (see [5, 11, 12, 17] and references therein). Following the practice in the pre-existing code, the ISRN is discretised on a coarse mesh which is further reconstructed around the grid of the reference CFD simulation. The latter allows for arbitrary positioning of the ISR reactors and facilitates data transfer between solvers by exploiting the topology of the CFD faces. In contrast with ideal reactor network approaches (e.g. [13]), clustering procedures are not required to identify chemically and physically homogeneous zones since ISRs are inhomogeneous in terms of their flow and mixture fraction fields. The current implementation also permits the use of parallel evaluation of reactors, hence speeding up computations.

The evaluation of core volume-averaged quantities and area-averaged fluxes requires knowledge about the mean flow and mixing fields. In this work, these quantities are extracted from previous CFD calculations of the Cambridge RQL combustor using LES-CMC and a detailed soot sectional model [5], as will be described later. CFD derived quantities, such as the mixture fraction PDF, are either evaluated at the faces of ISR reactors to calculate LHS terms of Eq. (6) or are directly accounted during volume-averaging. The interfacing procedure is similar to the one followed at every time-step of existing CMC codes (e.g. [17]). After the end of the calculation, unconditional quantities are derived through the integration of the mixture fraction PDF. Here, unconditional values are calculated at the CFD grid after applying an inverse square distance interpolation over neighbour ISR reactors. The PDF is here modelled with a presumed β-function computed from the mixture fraction, $\widetilde{\xi}$, and the mixture fraction variance, $\widetilde{\xi''^2}$ of each CFD cell. In case of singularities at the η-space boundaries, the β-function is replaced by a delta function.

The core-volume averaged scalar dissipation rate is obtained through Eq. (4). To calculate the conditional scalar dissipation rate at the CFD level, the Amplitude Mapping Closure (AMC) model [18] is employed, i.e. $\langle N|\eta\rangle = N_0 G_\eta$ where G_η and N_0 are $G_\eta = \exp(-2[\mathrm{erf}^{-1}(2\eta-1)]^2)$ and $N_0 = \widetilde{N}/\int_0^1 \widetilde{P_\eta} G_\eta d\eta$. The average scalar dissipation rate, $\widetilde{N}$, is readily available from the CFD simulation. It is important to note that in contrast with existing ISR models [6, 7, 8, 9], here, the core-volume averaged scalar dissipation rate is not based on the double integration of Eq. (5), raising issues of consistency with the PDF transport equation. Nonetheless, it has been observed that in a multi-dimensional system such as an ISRN, this approach may result in negative values of the scalar dissipation rate being obtained through numerical error [10]. Here, we preferred a more robust approach in evaluating the conditional scalar dissipation rate, which is also consistent with state-of-the-art CMC approaches (e.g. [17]).

An operator splitting technique is implemented for the solution of the ISRN equations. Transport in physical space, i.e. LHS terms of Eq. (6), are solved first, followed by diffusion in mixture fraction space and the chemical source term integration. The chemical source term is closed with a first-order approximation. A short description of the chemical mechanism and the soot model used in ths work is given in the following. A first-order upwind scheme is used for evaluation of conditional gradients, whereas the diffusion term in mixture fraction space is discretised with a second-order scheme. The inert mixing solution is imposed at the inlets and reactors are initialised with a fully-burning solution. Both walls and outlets are modelled with a zero-gradient condition. Consistently with the reference CFD simulations [5], mixture fraction space is discretised using 61 bins clustered around the stoichiometric mixture fraction ($\eta_{st} = 0.063$ for ethylene). Pure air is imposed at $\eta = 0$, whereas $\eta = 1$ corresponds to pure fuel. Ambient temperature, equal to 298K, is used for both boundaries and a constant pressure condition of 1 atm is used for all reactors.

CHEMICAL MECHANISM & SOOT MODEL

In this work, simulations are based on a detailed physicochemical model which has been developed and extensively tested by D'Anna and co-workers (see [19] and references therein). This model has been demonstrated to successfully predict soot formation for various fuels and flame configurations while supporting the latest experimental evidence of soot evolution in laminar flames [1, 2]. A simplified version of this approach has been recently presented in Ref. [5] and will be employed here. The detailed gas-phase mechanism includes pyrolysis/oxidation of hydrocarbons and considers the sequential addition of acetylene molecules and the self-combination of resonantly stabilised radicals to account for the molecular growth of aromatic cycles up to pyrene. All species with greater molecular mass are treated as lumped species and are divided into classes incorporated in the soot sectional model. Reactions for the lumped species and the gaseous-phase species involved in the soot model are treated as elementary reactions in accordance with the sectional approach.

Particle size distribution is defined by a single range of sections (bins), each containing a nominal hydrocarbon species in order of increasing atomic mass. Carbon number ranges from 24 to 2×10^{10}, which is equivalent to a mean mass diameter, D_{mm}, range of 0.8–630 nm assuming a constant soot particle density $\rho_s = 1800$ kg/m^3. Twenty-two sections are used in a geometric series with a carbon number ratio of, at least, two between sections. For each carbon number n_C, a stable (BIN) and a radical form (BIN*), i.e. a stable lumped species missing one H-atom, is used so that particles are classified both by their size and state. Other properties, such as hydrogen content, are extracted from the original version [19] of the model and are directly considered in the formulation of kinetic rates. All known physical and chemical pathways affecting soot evolution are included in the particle phase scheme and reactions are based on a modified Arrhenius expression with an additional dependency on the carbon number. The reactions classes consider: (i) particle inception via aromatics dimerisation, (ii) surface growth via C_2H_2, (iii) condensation of aromatics, (iv) oxidation via O_2 and OH, (v) particle coagulation via both coalescence and agglomeration, as well as (vi) O_2 oxidation-induced fragmentation. Overall, the lumped species mechanism contains 1763 reactions and 44 bins, whereas the gas-phase mechanism consists of 243 reactions and 67 species.

EXPERIMENTAL COMBUSTOR

The investigated combustor, developed at the University of Cambridge, is based on a bluff-body swirl-stabilized ethylene/air flame operating at atmospheric pressure. This configuration is able to reproduce the key features of a typical RQL gas-turbine combustor by allowing air to enter through three separate streams: (i) an inner swirling flow (primary air), located in the annular gap of the bluff body and generated by means of an axial swirler; (ii) a concentric swirling flow (secondary air), created through tangential ports in an annular chamber; (iii) four transverse jets at the burner's corners (dilution air). For more details regarding the burner and the experimental setup, the reader is addressed to Ref. [14]. A three-dimensional representation of the burner is also given in Fig. 1.

In this study, two operating conditions are investigated, sharing the same global equivalence ratio, $\phi_g = 0.36$, and fuel velocity, $U_f = 15.7$ m/s, but different mass flow ratio between the primary air and the transverse jets stream. Previous experimental [14, 15, 16] and numerical [5] studies in this burner have shown that these conditions drastically affect soot evolution and thereby, this study aims to replicate these findings. In case *A* (0% dilution), all the air mass is injected through the primary air stream with a

bulk velocity of $U_p = 13.0$ m/s. In case B (40% dilution), 40% of the air is equally split to the transverse jets, corresponding to four dilution air streams of 61.3 m/s, while the remaining part is injected through the primary air stream with $U_p = 7.9$ m/s. In both cases, the secondary air stream is deactivated, and the height of the transverse jets is $h = 47$ mm.

This combustor has been previously simulated using LES, the CMC combustion model and the detailed physicochemical sectional model described in the previous paragraph [5]. Figure 1 shows the time-averaged axial velocity for the two cases investigated in this study. The non-diluted case is characterised by a recirculation zone due to the combined effect of the bluff body, the swirling flow and the burner walls, whereas the diluted case is characterised by a recirculation zone confined below the transverse jets. Notably, with increasing dilution, the enhanced momentum of the transverse jets results in a stronger back-flow towards the bluff-body while reducing the penetration of the fuel jet. As discussed in Ref. [5, 11, 12], this has a significant effect on the local fuel-air-ratio and the mean residence time in the combustion chamber, significantly affecting soot evolution. Given the average flow and mixing field extracted from the LES-CMC results, the burner is then partitioned in 32 ISR reactors, reconstructed around the underlying CFD cells. Most reactors are located in the fuel-rich recirculation zone [5] to better resolve gradients in conditional soot related quantities. Additional reactors are located in the secondary region downstream to capture the soot burn-out. The sensitivity of the ISRN to reactor density will be investigated further in the final version of this study.

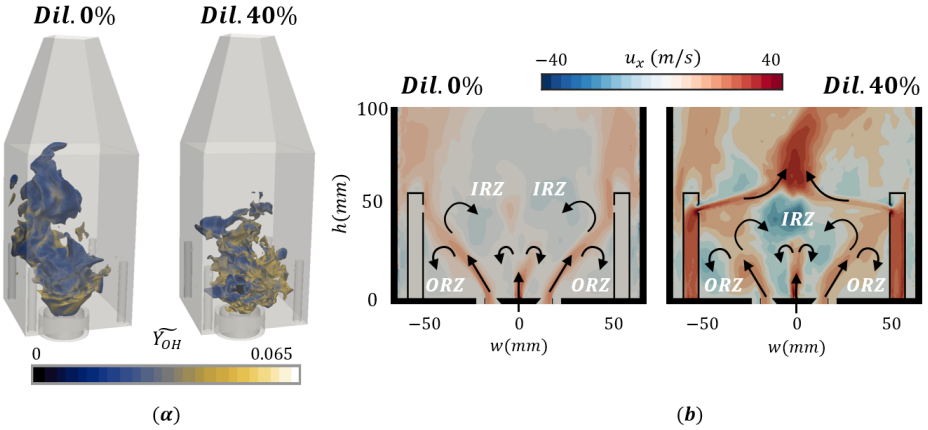

Figure 1: (a) Instantaneous iso-surface of the stoichiometric mixture fraction coloured with OH mass fraction for the two cases investigated in this work; (b) Time-averaged axial velocity of the reference LES-CMC simulations in a stream-wise cross section for the 0% dilution (left) and 40% dilution (right) cases.

RESULTS & DISCUSSION

Soot evolution has been experimentally investigated through qualitative LII measurements [15, 16]. In Fig. 2, the LII signal intensity is compared with the predicted soot volume fraction from the reference CFD and ISRN calculations. The comparison is aimed at assessing whether the simulations capture the measured location of soot presence and the relative magnitudes as dilution increases, as has also been performed in Ref. [5]. Without dilution air, the time-averaged LII signal was found to be persistent throughout the given field of view with higher concentrations near the bluff-body and inside the fuel-rich region of the primary zone, where the simulation predicts a significant reverse flow (see Fig. 1) and a favourable rich mixture fraction range for soot nucleation and growth to occur. On the contrary, when the dilution air is activated, the LII signal no longer persists downstream, and a drastic reduction in the signal occurs, at about the height of the transverse jets (h = 47 mm). These features, as well as the overall spatial distribution, are reasonably captured by both methods. The mean LII signal intensities reported here for the diluted case are lower by a factor of 16 compared to the non-diluted case. Further experiments are necessary to obtain quantitative information on the soot volume fraction; however, the latter depicts a decreasing trend in total soot production with additional dilution air. The simulations also capture this trend.

Differences between the two models are closely related to the evolution of conditional quantities. Figure 3 shows a representative comparison between the conditional averages as predicted by the ISRN (at steady-state) and the time-evolution of conditional quantities extracted from the LES-CMC. The high values of total soot mass, Y_s, may be explained by the location of the point of interest, P1, inside the inner recirculation zone, where residence time is sufficiently high to allow surface growth to occur, via acetylene (C_2H_2) and condensation of aromatics such as naphthalene (A2). It is essential to focus on the dispersion of the conditional mass fractions. This dispersion is primarily attributed to finite-rate chemistry and history effects induced by turbulent transport and large variation in micro-mixing through fluctuations of the scalar dissipation rate. Since these effects are considered within the ISRN, a good agreement in the predicted mean sooting flame structures is observed. The sensitivity of the ISRN approach to these effects is also relevant to the prediction of the soot particle size distribution (PSD). In Fig. 3, representative soot PSDs are considered at two locations inside the primary zone of the investigated non-diluted case. As shown by the comparison of the mean PSDs, the modelled soot PSDs show excellent agreement at point P1, similarly to the flame structure comparison, but differ significantly at point P2 which is located further downstream. This is probably attributed to an over-estimation of the residence time in the host reactor or an under-prediction of the conditional scalar dissipation rate.

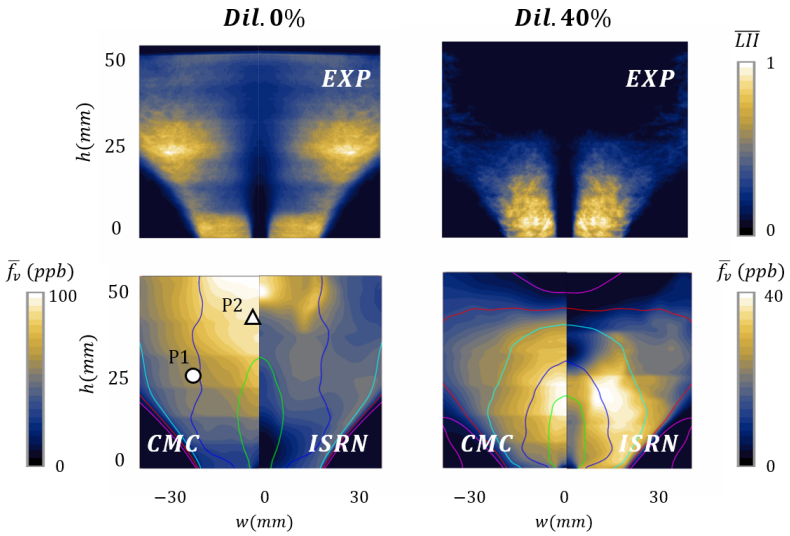

Figure 2: Comparison between experimental normalised mean LII signal intensity (top) and mean soot volume fraction as predicted by LES-CMC (bottom left-half plots) and ISRN (bottom right-half plots) for the two cases investigated in this study. Mean mixture fraction iso-lines: green=0.3, blue=0.2, cyan=0.12, red at stoichiometric and magenta at half the stoichiometric value. Locations P1-P2 are noted for further analysis.

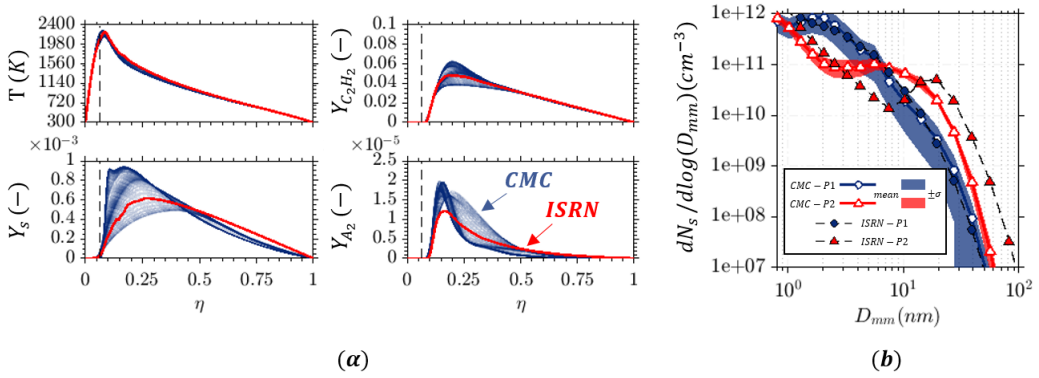

Figure 3: (a) Time evolution of LES-CMC conditional quantities vs the ISRN solution at a representative location P1 of the 0% dilution case. (b) Comparison of PSDs at two selected points of the 0% dilution case. ISRN simulation results (dashed lines) are compared with the mean LES-CMC simulation results (solid lines). The filled colour shows one standard deviation σ from the mean. See Fig. 2 for the location of points P1-P2.

Predictions are known to be sensitive to the choice of the soot model (see for example [3]) so more work is required to assess the predictability of other soot models given the same mixing field and choice of combustion models. Nevertheless, it is essential to note that the ISRN method appears to approximate well the results of the reference CFD cases and shows a very promising capability to perform kinetic post-processing and sensitivity analysis. Apart from the appropriate choice of the soot model and the fidelity of the mixing field, there is still space for improvement in the ISRN predictions. Future work will focus on the effects of the conditional scalar dissipation rate modelling, the grid sensitivity and the satisfaction of the ISR conditions at each reactor [10], as well as the inclusion of differential diffusion effects for soot particles.

As far as the implementation aspects of the ISRN are concerned, the method appears to be computationally very efficient. As the mixing field is pre-calculated and only a subset of processes is solved at each time-step, the computational cost is significantly minimized, allowing for the use of even more complex chemical mechanisms and soot models. Example average runtimes are given in Table 1. For the numerical setup presented here, a simulation of 10 ms (approximately one flow-through time [11, 12]) requires less than 24 h of physical time at a single supercomputer node. The current case appears to be limited by the interfacing between the ISR reactors and the reference CFD grid, due to the high dimensionality of the latter (about 20 million CFD cells). Naturally, further statistics are required to conclude the optimum number of reactors and ensure efficient load balancing.

CONCLUSIONS

A novel approach utilising an Incompletely Stirred Reactor Network (ISRN) approach has been introduced and formulated. An ISRN comprises of a network of stirred reactors which may be arbitrarily positioned and clustered around the mesh of a reference CFD simulation providing the average flow field. Due to its simplicity and low computational cost, this approach may be used

Table 1: Average runtime for advancing the ISRN model (32 ISRs, Naples soot model [5]) by one time step ($\Delta t = 2$ x 10^{-6}) on 1 node (32 MPI processes) of an Intel Xeon Skylake supercomputer (Cambridge CSD3).

Process	**Average runtime (s)**
CFD→ISRN interfacing	6.5
Transport in physical space	0.8
Transport in mixture fraction space	0.9
Chemistry integration	8.3
All processes	16.5

to explore soot evolution in aero-engine combustors utilising complex chemical mechanisms and comprehensive soot models that otherwise would be intractable to couple with current CFD methods. The ISRN approach has been demonstrated on two conditions of a model RQL combustor that have previously been calculated using LES, CMC and a detailed physicochemical soot sectional model. Results of soot distribution with the ISRN approach have been compared with experiments, showing promising potential in predicting soot emissions within a reasonable degree of accuracy while ensuring high computational efficiency. Further work and analysis are, however, required to validate the method further and study its sensitivity to modelling parameters.

ACKNOWLEDGEMENTS

The work presented in this abstract was supported by the UK Engineering and Physical Sciences Research Council (EPSRC) and Rolls-Royce plc. M. Sirignano and A. D'Anna from the University of Naples provided the chemical mechanism and sectional soot model used in this work. This is greatly acknowledged by the authors. The authors would also like to thank I. El Helou and A. W. Skiba for the useful discussions regarding the experiment and for providing the experimental data.

REFERENCES

[1] A. D'Anna. Combustion-formed nanoparticles. *Proc. Comb. Inst.*, 32(1):593–613, 2009.
[2] H. Wang. Formation of nascent soot and other condensed-phase materials in flames. *Proc. Comb. Inst.*, 33(1):41–67, 2011.
[3] S. T. Chong, V. Raman, M. E. Mueller, P. Selvaraj, and H. G. Im. Effect of soot model, moment method, and chemical kinetics on soot formation in a model aircraft combustor. *Proc. Comb. Inst.*, 37(1):1065 – 1074, 2019.
[4] M.A. Schiener and R.P. Lindstedt. *Proc. Comb. Inst.*, 37(1):1049 – 1056, 2019.
[5] S. Gkantonas, M. Sirignano, A. Giusti, A. D'Anna, and E. Mastorakos. Comprehensive Soot Particle Size Distribution Modelling Of A Model Rich-Quench-Lean Burner. In *11th Mediterannean Combustion Symposium, Tenerife, Spain*. June 2019.
[6] N.S.A. Smith. *Development of the conditional moment closure method for modelling turbulent combustion*. PhD thesis, University of Sydney, 1994.
[7] K. Mobini. *An investigation of the imperfectly stirred reactor modelling of recirculating combustion flows*. PhD thesis, University of Sydney, 1998.
[8] K. Mobini and R. W. Bilger. Imperfectly Stirred Reactor Model Predictions Of Reaction In A Burner With Strong Recirculation. *Combust. Sci. Technol.*, 176(1):45–70, 2004.
[9] K. Mobini and R.W. Bilger. Parametric study of the Incompletely Stirred Reactor modeling. *Combust. Flame*, 156(9):1818–1827, 2009.
[10] A.Y. Klimenko and R. W. Bilger. Conditional moment closure for turbulent combustion. *Prog. Energy Combust. Sci.*, 1999.
[11] A. Giusti, S. Gkantonas, J. M. Foale, and E. Mastorakos. Numerical Investigation of Flame Structure and Soot Formation in a Lab-Scale Rich-Quench-Lean Burner. (51067):V04BT04A032, 2018.
[12] S. Gkantonas, A. Giusti, and E. Mastorakos. A Numerical Study of Soot Evolution in a Lab-Scale Rich-Quench-Lean Burner. *Submitted to Flow Turbul. Combust.*, 2019.
[13] S. Lyra and R.S. Cant. Analysis of high pressure premixed flames using Equivalent Reactor Networks for predicting NOx emissions. *Fuel*, 107:261–268, 2013.
[14] T. E. Tracey, J. A. Sidey, and E. Mastorakos. In *AIAA SciTech Forum, paper 1880*, Kissimmee, Florida, USA, January 2018.
[15] I. El Helou, A. W. Skiba, E. Mastorakos, and J. A. Sidey. In *AIAA SciTech Forum, paper 1436*, San Diego, California, USA, January 2019.
[16] I. El Helou, A. W. Skiba, and E. Mastorakos. Investigation of Soot Production and Oxidation in A Lab-Scale Rich-Quench-Lean (RQL) Burner Using In-Situ Laser Diagnostics. In *11th Mediterannean Combustion Symposium, Tenerife, Spain*. June 2019.
[17] A. Giusti and E. Mastorakos. Detailed chemistry LES/CMC simulation of a swirling ethanol spray flame approaching blow-off. *Proc. Comb. Inst.*, 36(2):2625–2632, 2017.
[18] E. E. O'Brien and T. L. Jiang. The conditional dissipation rate of an initially binary scalar in homogeneous turbulence. *Phys. Fluids*, 3(12):3121–3123, 1991.
[19] M. Sirignano, J. Kent, and A. D'Anna. *Energy Fuels*, 27(4):2303–2315, 2013.